Journal of Molecular Structure 1106 (2016) 210–219

Contents lists available at ScienceDirect

Journal of Molecular Structure

journal homepage: http://www.elsevier.com/locate/molstruc

Synthesis, structure and cytotoxic activity of acetylenic derivatives of betulonic and betulinic acids

Ewa Bębenek [a, *], Elwira Chrobak [a], Joanna Wietrzyk [b], Monika Kadela [a], Artur Chrobak [c], Joachim Kusz [d], Maria Książek [c], Maria Jastrzębska [c], Stanisław Boryczka [a]

[a] Medical University of Silesia in Katowice, School of Pharmacy with the Division of Laboratory Medicine in Sosnowiec, Department of Organic Chemistry, 4 Jagiellonska Str., 41-200 Sosnowiec, Poland
[b] Polish Academy of Sciences, Ludwik Hirszfeld Institute of Immunology and Experimental Therapy, Department of Experimental Oncology, 12 R. Weigla Str., 53-114 Wrocław, Poland
[c] University of Silesia, Institute of Physics, Department of Solid State Physics, 4 Uniwersytecka Str., 40-007 Katowice, Poland
[d] University of Silesia, Institute of Physics, Department of Physics of Crystals, 4 Uniwersytecka Str., 40-007 Katowice, Poland

ARTICLE INFO

Article history:
Received 5 October 2015
Accepted 30 October 2015
Available online 4 November 2015

Keywords:
Betulonic acid
Betulinic acid
Acetylenic derivatives
Crystal structure
Cytotoxic activity
DSC

ABSTRACT

A series of acetylenic derivatives of betulonic and betulinic acids has been synthesized and characterized by ^{1}H and ^{13}C NMR, IR and MS spectroscopy. The structure of propargyl betulonate **4** and propargyl betulinate-DMF solvate **8A** was solved by X-ray diffraction. Thermal properties were examined using a DSC technique. The resulting alkynyl derivatives, as well as betulin **1** and betulinic acid **3**, were evaluated *in vitro* for their cytotoxic activity against human T47D breast cancer, CCRF/CEM leukemia, SW707 colorectal, murine P388 leukemia and BALB3T3 normal fibroblasts cell lines. Several of the obtained compounds have a favorable cytotoxic profile than betulin **1**. Propargyl betulinate **8** was the most active derivative, being up to 3-fold more potent than betulin **1** against the human leukemia (CCRF/CEM) cell line, with an IC_{50} value of 3.9 μg/mL.

1. Introduction

Betulin **1**, betulonic acid **2** and betulinic acid **3** are pentacyclic triterpenes of the lupane type, which were isolated from birch bark (*Betula alba*, *Betula pendula*, *Betula pubescent* and *Betula platyphylla*) and other various plants [1,2]. Betulin [lup-20(29)-ene-3β,28-diol] **1** is a major constituent of the bark of white birches (up to 30%). Compound **1** is usually modified at C28, C3 and C20 positions giving derivatives, which show a wide spectrum of biological activities such as anticancer, antiviral, antibacterial, anti-inflammatory, antiseptic and anti-leishmanial (Fig. 1) [3,4].

Betulin **1** can be oxidized with the Jones reagent to betulonic acid **2**, which then can be selectively reduced with $NaBH_4$ to more water-soluble betulinic acid **3** [5,6]. An increase in biological activity of betulonic acid **2** and betulinic acid **3** derivatives was obtained via esterification of the C17 carboxyl group [7,8]. It was reported in the previous studies on betulin derivatives that the introduction of an alkynyl group is favorable for improvement of biological activity [9]. Acetylenic derivatives of betulin have anticancer and antiviral properties, therefore we have focused on the synthesis of new betulonic and betulinic acids derivatives containing an alkynyl moiety [9–12]. Derivatives of betulin exhibit a great ability to form solvates with different organic solvents [13,14]. The occurrence of biologically active compounds in the form of solvatomorphs affects their properties such as solubility, stability, density and bioavailability [15,16]. Boryczka et al. [17,18] reported the crystal structures of betulonic acid **2** (DMSO and DMF) and betulinic acid **3** (DMSO) solvates. In the present work, we described the synthesis of new alkynyl derivatives of betulonic and betulinic acids. In addition, the structures of two esters were confirmed by X-ray analysis. All synthesized compounds were tested for cytotoxic activity against human: breast cancer (T47D), leukemia (CCRF/CEM), colorectal adenocarcinoma (SW707), and murine: leukemia (P388) as well as normal fibroblasts (BALB3T3) cell lines.

* Corresponding author.
E-mail address: ebebenek@sum.edu.pl (E. Bębenek).

http://dx.doi.org/10.1016/j.molstruc.2015.10.102
0022-2860/

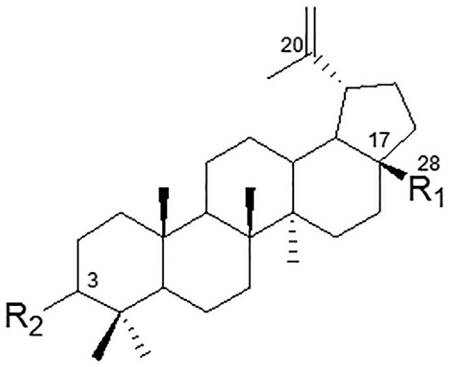

Betulin **1** $R_1 = CH_2OH$, $R_2 = OH$
Betulonic acid **2** $R_1 = COOH$, $R_2 = O$
Betulinic acid **3** $R_1 = COOH$, $R_2 = OH$

Fig. 1. Structure of betulin **1**, betulonic acid **2** and betulinic acid **3**.

2. Experimental

2.1. Methods and materials

Melting points of compounds were obtained in open capillary tubes on a Boetius melting point apparatus without correction. NMR (600/150 MHz) spectra were measured on a Bruker MSL 600 spectrometer in $CDCl_3$ with tetramethylsilane (Me_4Si) as internal standard. Chemical shifts values are reported in ppm (δ) and the coupling constants (J) are presented in Hertz. Multiplicity is designated as singlet (s), doublet (d), triplet (t) and multiplet (m). Mass spectra were measured under EI conditions on a Finnigan MAT 95 spectrometer. Infrared spectra (KBr, pellet) were recorded using the IRAffinity-1 Shimadzu spectrometer. The progress of reactions were monitored by TLC on silica gel 60 254F plates using a mixture of chloroform and ethanol (40:1 and 20:1, v/v) as an eluent. Spots were developed by spraying with a solution of 5% sulfuric acid and heating to 100 °C. Purification of the compounds was carried out by column chromatography (silica gel 60, <63 μm, Merk) using a mixture of chloroform and ethanol (40:1, v/v) as an eluent. All reactions solvents were dried and purified according to usual procedures.

2.1.1. Synthesis of betulonic acid *2*

The bark (100 g) of the white birch (*Betula verrucosa*), collected in Poland, was cut into small pieces, soaked in dichloromethane (1 L) and refluxed for 8 h. The solvent was removed under reduced pressure to produce a yellow product. The crude betulin **1** was purified by column chromatography (chloroform/ethanol, 20:1, v/v) to give pure compound **1** as a white solid (19 g, 19%): mp 250–252 °C (lit. [19], 252–253 °C); R_f 0.42 (chloroform/ethanol, 20:1, v/v). Betulin **1** was oxidized with the Jones reagent (CrO_3/H_2SO_4/0 °C) in acetone to give betulonic acid **2** in 75% yield (Scheme 1) according to the method described by Kim [5]. Betulonic acid **2** was purified by column chromatography using a mixture of chloroform and ethanol (40:1, v/v) as an eluent: mp 256–258 °C (lit. [20], 258 °C); R_f 0.34 (chloroform/ethanol, 40:1, v/v).

2.1.2. General procedure for the synthesis of derivatives *4–6*

The chemical structures of compounds **4**, **8** and **11** were determined using ^1H, ^{13}C NMR, IR and MS spectroscopy and the assignments were done based on the literature [21–23].

Betulonic acid **2** 0.15 g (0.33 mmol) was dissolved in dry *N*,*N*-dimethylformamide (2.3 mL) and the solution was stirred at room temperature. Then, 0.14 g (1 mmol) of anhydrous potassium carbonate and 0.7 mmol of propargyl bromide, 1-bromo-2-butyne or 1-bromo-3-butyne were added to the reaction mixture and stirred at this temperature for 1 h. At the end of the reaction 15 mL of dichloromethane was added and the organic layer was washed twice with 10% hydrochloric acid and once with saturated sodium hydrogencarbonate. The organic layer was dried with anhydrous magnesium sulfate and concentrated under reduced pressure. The crude products were purified by column chromatography (SiO_2, eluent: chloroform/ethanol, 40:1, v/v) to give pure compounds **4–6**.

2-Butynyl betulonate **5**. Yield 81%; mp 172–174 °C; R_f 0.63 (chloroform/ethanol, 40/1, v/v). ^1H NMR ($CDCl_3$): δ = 0.92 (3H, s, CH_3), 0.97 (3H, s, CH_3), 0.98 (3H, s, CH_3), 1.02 (3H, s, CH_3), 1.07 (3H, s, CH_3), 1.17–2.48 (23H, m, CH, CH_2), 1.69 (3H, s, CH_3), 1.85 (3H, t, J = 2.4 Hz, CCH_3), 3.02–3.06 (1H, m, 19-H), 4.61 (1H, s, 29-H), 4.66–4.73 (2H, m, OCH_2), 4.74 (1H, s, 29-H) ppm. ^{13}C {^1H} NMR ($CDCl_3$): δ = 3.7, 14.6, 15.7, 15.9, 19.4, 19.7, 21.0, 21.4, 25.6, 26.6, 29.6, 30.5, 31.9, 33.6, 34.1, 36.8, 36.9, 38.3, 39.6, 40.7, 42.5, 46.8, 47.3, 49.5, 49.9, 52.1, 55.0, 56.5, 73.6, 82.4, 109.6, 150.5, 175.4, 218.1 ppm. IR (KBr) ν = 2837–2976 (CH), 2237 (C≡CH), 1723 (C=O), 1152 (C–O) cm^{-1}. Mass spectrum m/z (EI, 70eV) m/z (rel. int.) = 507 (M^+, 17%), 409 (46), 203 (42), 189 (100).

3-Butynyl betulonate **6**. Yield 56%; mp 77–79 °C; R_f 0.63 (chloroform/ethanol, 40/1, v/v). ^1H NMR ($CDCl_3$): δ = 0.92 (3H, s, CH_3), 0.96 (3H, s, CH_3), 0.98 (3H, s, CH_3), 1.02 (3H, s, CH_3), 1.07 (3H, s, CH_3), 1.15–2.51 (23H, m, CH, CH_2), 1.69 (3H, s, CH_3), 1.99 (1H, t, J = 2.4 Hz, CCH), 2.53–2.55 (m, 2H, OCH_2CH_2), 3.01–3.03 (1H, m, 19-H), 4.18–4.22 (m, 2H, OCH_2CH_2), 4.61 (1H, s, 29-H), 4.74 (1H, s, 29-H) ppm. ^{13}C {^1H} NMR ($CDCl_3$): δ = 14.6, 15.8, 15.9, 19.1, 19.4, 19.6, 21.0, 21.4, 25.5, 26.6, 29.6, 30.6, 32.0, 33.6, 34.1, 36.9, 37.0, 38.4, 39.6, 40.7, 42.5, 46.9, 47.3, 49.4, 49.9, 55.0, 56.6, 61.6, 69.8, 80.3, 109.6, 150.5, 175.9, 218.1 ppm. IR (KBr) ν = 3311 (C≡CH), 2869–2963 (CH), 2123 (C≡C), 1729 (C=O), 1261 (C–O) cm^{-1}. Mass spectrum (EI, 70eV) m/z (rel. int.) = 507 (M^+, 18%), 409 (42), 203 (37), 189 (100).

2.1.3. General procedure for the synthesis of derivative *7*

A solution of betulonic acid **2** 0.15 g (0.33 mmol) in dry dichloromethane (4.8 mL) and oxalyl chloride 0.06 g (0.5 mmol) was stirred at room temperature for 24 h. The reaction mixture was concentrated under reduced pressure and the solid was treated with cyclohexane (3.4 mL), which was then removed. This procedure was repeated twice to yield 0.12 g of crude betulonoyl chloride. A solution of propargylamine 0.02 g (0.37 mmol) and triethylamine 0.07 g (0.73 mmol) in dichloromethane (1.0 mL), was added to a solution of betulonoyl chloride in dry dichloromethane (3.5 mL). This reaction mixture was stirred at room temperature for 24 h. At the end of the reaction 7.5 mL of dichloromethane was added and the organic layer was washed twice with water, then dried with anhydrous magnesium sulfate and concentrated under reduced pressure. The crude product was purified by column chromatography (SiO_2, eluent: chloroform/ethanol, 40:1, v/v) to give pure compound **7**.

N-propargyl amide of betulonic acid **7**. Yield 71%; mp 116–118 °C; R_f 0.55 (chloroform/ethanol, 40/1, v/v). ^1H NMR ($CDCl_3$): δ = 0.92 (3H, s, CH_3), 0.97 (3H, s, CH_3), 0.98 (3H, s, CH_3), 1.01 (3H, s, CH_3), 1.06 (3H, s, CH_3), 1.16–2.46 (23H, m, CH, CH_2), 1.68 (3H, s, CH_3), 2.21 (1H, t, J = 2.4 Hz, CCH), 3.11–3.14 (1H, m, 19-H), 4.06–4.08 (2H, m, OCH_2), 4.59 (1H, s, 29-H) 4.74 (1H, s, 29-H), 5.72 (1H, t, J = 4.9 Hz, NH) ppm. ^{13}C {^1H} NMR ($CDCl_3$): δ = 14.5, 15.8, 15.9, 19.5, 19.6, 21.0, 21.4, 25.6, 26.5, 28.9, 29.3, 30.7, 33.5, 33.6, 34.1, 36.9, 36.9, 37.7, 38.1, 39.6, 40.7, 42.5, 46.6, 47.3, 49.9, 50.1, 55.0, 55.6, 71.1, 80.1, 109.4, 150.7, 175.8, 218.2 ppm. IR (KBr) ν = 3311 (C≡CH), 2867–2954 (CH), 2116 (C≡CH), 1704 (C=O), 1516 (NH) cm^{-1}. Mass spectrum (EI, 70eV) m/z (rel. int.) = 492 (M^+, 39%), 409 (82), 272 (59), 189 (79).

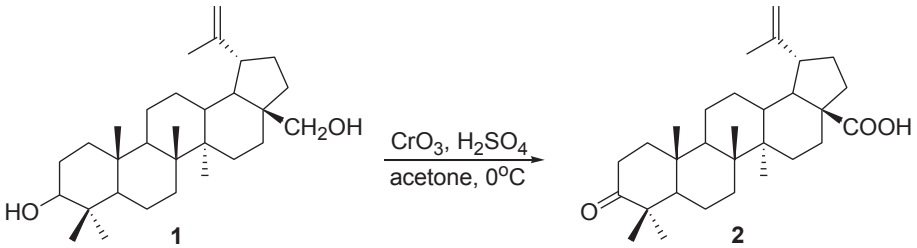

Scheme 1. Synthesis of betulonic acid **2**.

*2.1.4. General procedure for the synthesis of derivatives **8**–**11***

Sodium tetrahydroborate 0.4 g (1.1 mmol) was added to a mixture of derivatives **4**–**7** (0.33 mmol) in dry tetrahydrofuran (10 mL) and the reaction was stirred at room temperature for 24 h. At the end of the reaction 7 mL of water was added and the reaction mixture was extracted with dichloromethane (2 × 5 mL). The organic layer was separated, then dried with anhydrous magnesium sulfate and concentrated under reduced pressure. The crude products were purified by column chromatography (SiO_2, eluent: chloroform/ethanol, 40:1, v/v) to give pure compounds **8**–**11**.

Propargyl betulinate **8A**. Recrystallization from DMF-acetone solution (1:10, v/v); mp 118–120 °C.^{1}H NMR ($CDCl_3$) δ = 0.75 (3H, s, CH_3), 0.81 (3H, s, CH_3), 0.92 (3H, s, CH_3), 0.95 (3H, s, CH_3), 0.96 (3H, s, CH_3), 0.86–2.30 (24H, m, CH, CH_2), 1.68 (3H, s, CH_3), 2.43 (1H, t, J = 2.4 Hz, CCH), 2.88 (3H, s, NCH_3), 2.95 (3H, s, NCH_3), 2.98–3.03 (1H, m, 19-H), 3.15–3.19 (1H, m, 3-H), 4.59 (1H, s, 29-H), 4.61–4.72 (2H, m, OCH_2), 4.73 (1H, s, 29-H), 8.01(1H, s, CH from DMF) ppm. ^{13}C {^{1}H} NMR ($CDCl_3$) δ = 14.7, 15.4, 16.0, 16.1, 18.3, 19.4, 20.9, 25.5, 27.4, 28.0, 29.6, 30.5, 31.5, 32.0, 34.3, 36.4, 36.8, 37.2, 38.3, 38.7, 38.9, 40.8, 42.4, 46.9, 49.5, 50.6, 51.3, 55.4, 56.6, 74.3, 78.1, 79.0, 109.7, 150.5, 162.5, 175.2 ppm.

2-Butynyl betulinate **9**. Yield 68%; mp 156–158 °C; R_f 0.24 (chloroform/ethanol, 40/1, v/v). ^{1}H NMR ($CDCl_3$): δ = 0.75 (3H, s, CH_3), 0.82 (3H, s, CH_3), 0.94 (3H, s, CH_3), 0.96 (3H, s, CH_3), 0.97 (3H, s, CH_3), 1.18–2.29 (24H, m, CH, CH_2), 1.68 (3H, s, CH_3), 1.84 (3H, t, J = 2.4 Hz, CCH_3), 2.99–3.04 (1H, m, 19-H), 3.17–3.19 (1H, m, 3-H), 4.60 (1H, s, 29-H), 4.65–4.69 (2H, m, OCH_2), 4.74 (1H, s, 29-H) ppm. ^{13}C {^{1}H} NMR ($CDCl_3$): δ = 3.6, 14.7, 15.3, 15.9, 16.1, 18.3, 19.4, 20.9, 25.5, 27.4, 27.9, 29.6, 30.5, 32.0, 34.3, 36.8, 37.2, 38.3, 38.7, 38.9, 40.7, 42.4, 46.9, 49.5, 50.6, 52.1, 55.4, 56.5, 73.7, 78.9, 82.4, 109.6, 150.6, 175.4 ppm. IR (KBr) ν = 3388 (OH), 2870–2942 (CH), 2238 (C≡C), 1730 (C=O), 1123 (s, C–O). Mass spectrum (EI, 70eV) m/z (rel. int.) = 508 (M^+, 43%), 410 (76), 207 (51), 189 (100) cm^{-1}.

3-Butynyl betulinate **10**. Yield 69%; mp 102–105 °C; R_f 0.25 (chloroform/ethanol, 40/1, v/v). ^{1}H NMR ($CDCl_3$): δ = 0.75 (3H, s, CH_3), 0.82 (3H, s, CH_3), 0.92 (3H, s, CH_3), 0.96 (3H, s, CH_3), 0.97 (3H, s, CH_3), 1.13–2.01 (24H, m, CH, CH_2), 1.68 (3H, s, CH_3), 2.20–2.25 (m, 2H, OCH_2CH_2), 2.54 (1H, t, J = 2.4 Hz, CCH), 3.00–3.02 (1H, m, 19-H), 3.17–3.19 (m, 1H, 3-H), 4.12–4.20 (m, 2H, OCH_2CH_2), 4.60 (1H, s, 29-H), 4.73 (1H, s, 29-H) ppm. ^{13}C {^{1}H} NMR ($CDCl_3$): δ = 14.3, 14.7, 15.3, 16.1, 18.3, 19.1, 20.9, 21.0, 25.6, 27.4, 28.0, 29.6, 30.6, 32.2, 34.3, 37.0, 38.3, 38.9, 40.7, 42.4, 47.0, 49.4, 50.6, 55.4, 56.4, 56.6, 59.8, 61.6, 69.7, 79.0, 80.3, 109.6, 150.6, 175.9 ppm. IR (KBr) ν = 3423 (OH), 3312 (C≡CH), 2869–2944 (CH), 2123 (C≡C), 1724 (C=O), 1263 (C–O). Mass spectrum (EI, 70eV) m/z (rel. int.) = 508 (M^+, 12%), 411 (32), 207 (47), 189 (100) cm^{-1}.

3. Crystal structure determination

3.1. X-ray diffraction experiment

The single-crystal X-ray experiments were performed at 100K. For this measurement, colorless single crystals of good quality were preselected under a polarized light microscope. The crystals were mounted on a quartz capillary. The data were collected using an Oxford Diffraction diffractometer with Sapphire 3 CCD detector. Accurate cell parameters were determined and refined using CrysAlis CCD program [24]. For the integration of the collected data, the CrysAlis RED program [24] was used.

The crystal structures have been deposited in the Cambridge Crystallographic Data Centre and allocated the deposition numbers: CCDC 1050588 for **4** and 1050589 for **8A**.

3.1.1. Refinement

The structure were solved using direct method with SHELXS-2014 [25] program and then the solutions were refined using SHELXL-2014 [25] program. H atoms were treated as riding atoms in geometrically idealized positions, fixing the C–H bond lengths at 0.95, 1.00, 0.99, 0.95 and 0.98 Å for aldehyde CH, methine CH, methylene CH_2, terminal methylene CH_2 and methyl CH_3 atoms respectively, and with Uiso(H) = 1.5Ueq(C) for methyl H atoms or 1.2Ueq(C) otherwise. Hydrogen atoms involved in H-bonding (acetylenic and hydroxyl H atoms) were introduced into the calculated positions and then refined freely with isotropic atomic displacement parameters.

3.2. Differential scanning calorimetry (DSC)

Thermal analysis was performed with the differential scanning calorimetry (DSC, Perkin Elmer, DSC-7) in the temperature range from room temperature to 220 °C and heating rate 20 K/min.

3.3. Antyproliferative assay in vitro

Study of cytotoxic activity *in vitro* was performed using the following cell lines: T47D (human breast cancer), CCRF/CEM (human leukemia), SW707 (human colorectal), P388 (mouse leukemia) and BALB3T3 (normal mouse fibroblasts). All tested cell lines were obtained from the American Type Culture Collection (Rockville, MD, USA) and maintained at the Cell Culture Collection of the Institute of Immunology and Experimental Therapy (Wrocław, Poland). Twenty-four hours before addition of the obtained compounds the cells were plated in 96-well plates (Sarstedt, Numbrecht, Germany) at a density of 10^4 cells per well in 100 μL of culture medium. The cells were cultured in the opti-MEM medium supplemented with 2 mM glutamine (Gibco, Grand Island, NY, USA), streptomycin (50 μg/mL), penicillin (50 U/mL) (both antibiotics from Polfa, Tarchomin, Poland) and 5% fetal calf serum (Gibco). The cell cultures were maintained at 37 °C in atmosphere saturated with 5% CO_2. The alkynyl derivatives, as well as betulin **1** and betulinic acid **3** were dissolved in DMSO and culture medium (1:9) to the concentration of 1 mg/mL, and next diluted in culture medium to reach the required concentrations (ranging from 1 to 100 μg/mL). The *in vitro* cytotoxic effect of all compounds was

examined using the SRB assay for adherent cells and MTT assay for leukemia cells as described by Wietrzyk [26]. All tested compounds in given concentration were examined in triplicates in each experiment, which was repeated 3–5 times. The results of antiproliferative activity *in vitro* were expressed as an IC_{50} in μg/mL.

4. Results and discussion

4.1. Synthesis

Betulin **1** was the starting material used directly for the synthesis of betulonic acid **2**, according to the method described in the literature (Scheme 1) [5]. The purified compound **1** was oxidized with the Jones reagent (CrO_3/H_2SO_4/0 °C) in acetone giving **2** in 75% yield. The chemical structure of betulonic acid **2** was confirmed using ^1H and ^{13}C NMR and IR spectroscopy and then compared with the spectral data described in the literature [20,27].

The treatment of betulonic acid with propargyl bromide, 1-bromo-2-butyne or 1-bromo-3-butyne in *N*,*N*-dimethylformamide (DMF) in the presence of potassium carbonate (K_2CO_3) at room temperature gave esters **4**–**6** in 56–81% yields. The reaction of betulonic acid **2** with oxalyl chloride in dichloromethane gave betulonoyl chloride, which was immediately used in the reaction with propargylamine in dichloromethane in the presence of triethylamine to produce acetylenic derivative **7** in 71% yield. Reduction of acetylenic derivatives of betulonic acid **4**–**7** with sodium tetrahydroborate ($NaBH_4$) in tetrahydrofuran (THF) led to the formation of compounds **8**–**11** in 68–75% yields. The new compounds were purified by column chromatography using a mixture of chloroform and ethanol as an eluent. The chemical structure of all acetylenic derivatives **4**–**11** were determined on the basis of their ^1H, ^{13}C NMR, IR and MS spectra. Additionally, compounds **4** and **8** were examined by X-ray diffraction and DSC analysis. The synthesis of acetylenic derivatives of betulonic and betulinic acids was carried out according to Scheme 2.

4.2. X-ray structural studies

Due to the significant influence of various intra- and intermolecular interactions on the properties of medicinal substances such as stability, solubility and bioavailability, the knowledge of molecular structure of new bioactive compounds is very important [15,28]. Moreover, the previously described tendency of betulin derivatives to form solvates with various solvents indicates the need of study the novel compounds also in this respect. In this work, two propargyl derivatives **4** and **8** were examined by X-ray diffraction. Single crystals, suitable for the X-ray analysis, were grown by slow evaporation from the DMF-acetone saturated solution (1:10, v/v), under ambient conditions. Details of the performed X-ray analyses are summarized in Table 1. During crystallization of betulinic acid derivative **8**, incorporation of solvent molecules occurred. Finally, propargyl betulinate **8** was isolated as DMF solvate, denoted as **8A**. Molecular structures with atom and ring numbering for both crystals are presented in Fig. 2. The unit cell of **4** contains four molecules of propargyl betulonate **4** (Z' = 4), while **8A** contains four molecules **8** and DMF (Z' = 4) (Table 2).

In both crystals (**4** and **8A**), six membered rings (A, B, C, D) (for ring numbering see Fig. 2) adopt chair conformation and all the ring junctions in the pentacyclic system are trans-fused. The methyl groups with C24, C25, C26 and C27 atoms occupy axial positions, while that with C23 is equatorial.

The chair-conformation of cyclohexanone A-ring, in the propargyl betulonate **4** crystal, is similar to that found in lupenon [29], in betulonic aldehyde [30] but different to those described for the DMF and DMSO solvatomorphs of betulonic acid [18] where the A-ring adopts a twisted-boat conformation. The carbonyl group at the position C3 is in the coplanar orientation with C2–C3–C4 plane of the A-ring. The oxygen atom O1 deviates from this plane by 0.027 Å. In a contrast to solvates of betulonic acid [18], in the crystal of ester **4**, the carbonyl group C3 = O1 is not involved in the creation of the classic strong hydrogen bonds, which could affect the conformation and therefore the A-ring adopts the most stable chair conformation.

The A-ring of crystal 8A also adopts the chair-conformation, as in the previously described solvates of betulin [19,31], betulinic acid [17,32], lupeol [33] and betulinic acid benzyl ester [34]. The hydroxyl group located at the C3 carbon atom is in the equatorial position. The torsion angle, characterizing orientation of this group (O1–C3–C4–C5) is −177.53° and is similar to the corresponding

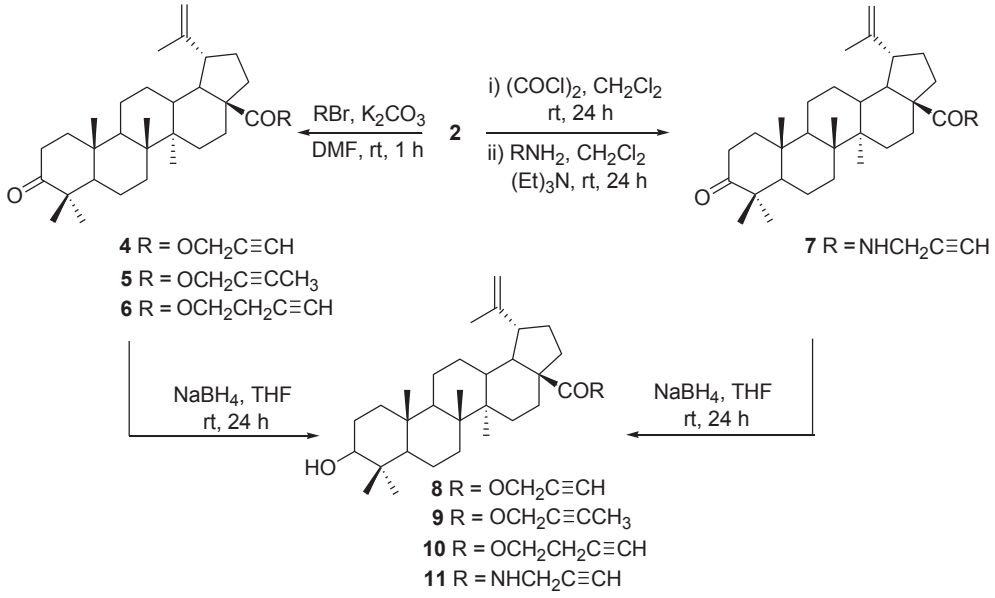

Scheme 2. Synthesis of acetylenic derivatives of betulonic and betulinic acid **4**–**11**.

Table 1
Experimental details.

	4	**8A**
Crystal data		
Chemical formula	$C_{33}H_{48}O_3$	$C_{33}H_{50}O_3 \cdot C_3H_7NO$
M_r	492.71	567.82
Crystal system, space group	Orthorhombic, $P2_12_12_1$	Orthorhombic, $P2_12_12_1$
Temperature (K)	100	
a, b, c (Å)	8.3645 (1), 15.3330 (2), 21.4695 (4)	7.0295 (2), 16.0757 (5), 28.4074 (9)
V (Å^3)	2753.53 (7)	3210.15 (17)
Z	4	
Radiation type	Mo $K\alpha$	
μ (mm^{-1})	0.07	0.08
Crystal size (mm)	0.60 × 0.12 × 0.06	0.60 × 0.08 × 0.07
Data collection		
Diffractometer	Oxford diffraction diffractometer with Sapphire3 detector	
Absorption correction	Multi-scan *CrysAlis RED*, Oxford diffraction Ltd., Version 1.171.32.29 empirical absorption correction using spherical harmonics, implemented in SCALE3 ABSPACK scaling algorithm.	
T_{min}, T_{max}	0.859, 1.000	0.617, 1.000
No. of measured, independent andobserved [$I > 2\sigma(I)$] reflections	18533, 4866, 4292	22205, 5684, 4502
R_{int}	0.029	0.044
(sin $\theta/\lambda)_{max}$ (Å^{-1})	0.596	0.596
Refinement		
$R[F^2 > 2\sigma(F^2)]$, $wR(F^2)$, S	0.030, 0.071, 0.90	0.036, 0.072, 0.90
No. of reflections	4866	5684
No. of parameters	359	411
H-atom treatment	H atoms treated by a mixture of independent and constrained refinement	
$\Delta\rangle_{max}$, $\Delta\rangle_{min}$ (e Å^{-3})	0.16, −0.17	0.16, −0.17
Absolute structure	Flack × determined using 1743 quotients [(I+)-(I-)]/[(I+)+(I-)] (Parsons, Flack and Wagner, Acta Cryst. B69 (2013) 249–259).	Flack × determined using 1676 quotients [(I+)-(I-)]/[(I+)+(I-)] (Parsons, Flack and Wagner, Acta Cryst. B69 (2013) 249–259).
Absolute structure parameter	−0.1 (3)	1.5 (6)

angle in the betulinic acid-DMSO solvate crystal (−179.26°) and betulin-DMSO (−176.5°) [17,19].

In both crystals, the cyclopentane E-ring adopts an envelope conformation with the C17 atom being displaced from the C18–C19–C21–C22 plane by about 0.635 Å in **4** and 0.652 Å in **8A**.

The most important conformational difference between the crystal structures of **4** and **8A** is the orientation of the ester group attached to atom C17 of the D-ring (see Fig. 3). The arrangement of this group can be described by following torsion angles: O2–C28–C17–C18 and C32–C31–O3–C28, which are equal to −21.01°, 177.93° for **4**, and 156.09°, −84.30° for **8A**, respectively.

A similar arrangement of substituents at the position C17, in relation to **4**, has been described for betulinic acid benzyl ester [34], methyl 3β-N-(t-butoxycarbonyl)-3-deoxybetulinate [35] and for 3-

Table 2
Selected geometric parameters.

Distance (Å) angle (degree)	4	8A	Angle (degree)	4	8A
O1–C3	1.216(2)	1.438(3)	O1–C3–C4–C5	129.9(2)	−177.5(2)
O3–C28	1.352(2)	1.345(3)	O1–C3–C4–C2	178.5(3)	−124.3(3)
O2–C28	1.205(2)	1.203(3)	C1–C2–C3–O1	−124.6(2)	179.8(2)
C17–C28	1.527(2)	1.537(3)	C18–C19–C20–C29	131.5(2)	137.8(2)
C17–C22	1.546(2)	1.551(3)	C21–C19–C20–C29	−111.1(2)	−104.6(3)
C17–C18	1.536(2)	1.537(3)	C18–C19–C20–C30	−50.9(2)	−46.4(3)
C18–C19	1.541(2)	1.551(3)	C21–C19–C20–C30	66.5(2)	71.2(3)
C19–C20	1.514(3)	1.517(3)	C16–C17–C28–O3	40.8(2)	−151.5(2)
C19–C21	1.568(3)	1.570(4)	C16–C17–C28–O2	−142.0(2)	32.9(3)
C20–C29	1.320(3)	1.319(4)	C22–C17–C28–O3	−88.4(2)	83.0(2)
C20–C30	1.493(3)	1.507(4)	C22–C17–C28–O2	88.8(2)	−92.7(3)
			C18–C17–C28–O3	161.7(2)	−28.2(3)
O1–C3–C2	120.9(1)	111.4(2)	C18–C17–C28–O2	−21.0(3)	156.1(2)
O1–C3–C4	121.8(2)	108.8(2)	C32–C31–O3–C28	177.9(2)	−84.3(3)
C20–C19–C18	114.8(2)	116.3(2)	C2–C1–C10–C5	54.4(2)	50.4(3)
C20–C19–C21	111.3(2)	111.4(2)	C1–C10–C5–C4	−52.4(2)	−50.7(3)
C29–C20–C30	121.1(2)	121.0(3)	C2–C3–C4–C5	−48.6(2)	−53.3(3)
C29–C20–C19	121.3(2)	121.0(2)	C1–C2–C3–C4	54.0(2)	57.0(3)
C2–C3–C4	117.3(2)	113.0(2)	C17–C18–C19–C21	23.2(2)	25.4(2)
O2–C28–C17	110.6(2)	114.0(2)	C19–C21–C22–C17	−27.4(2)	−26.0(3)
O2–C28–O3	122.3(2)	122.4(2)	O1–C2–C3–C4	178.5(3)	−122.8(3)
O3–C28–C17	127.1(2)	123.4(2)	O1–C2–C3–C24	−145.4(2)	−89.5(2)
C30–C20–C19	117.5(2)	117.9(2)			
C16–C17–C28	110.5(2)	108.2(2)			
C28–C17–C22	106.5(2)	106.9(2)			

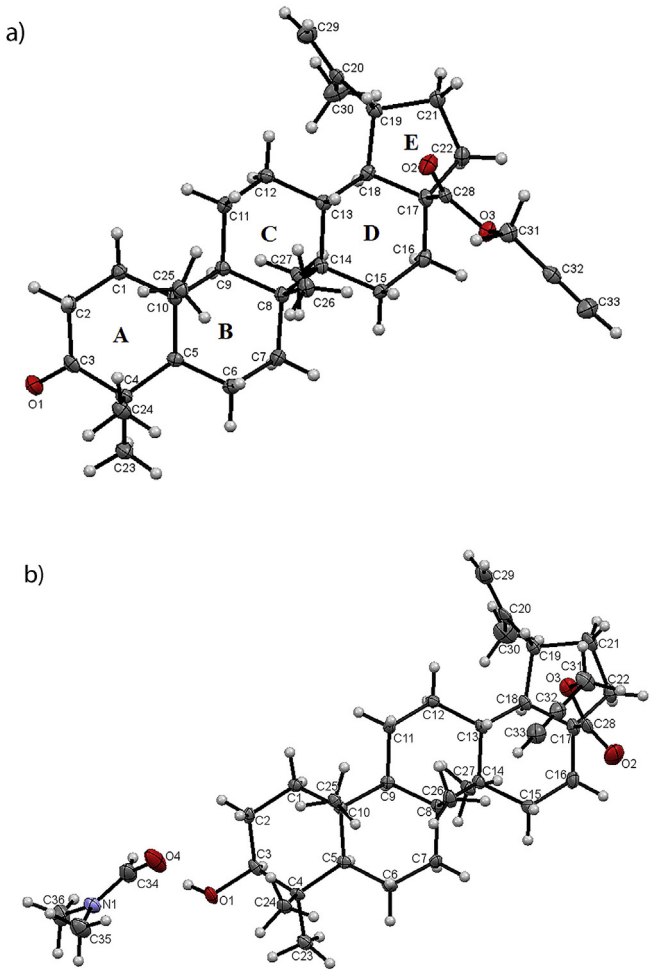

Fig. 2. Molecular structures with atom numbering of propargyl betulonate **4** (a) and propargyl betulinate *N*,*N* dimethylformamide solvate **8A** (b).

allyl betulinic acid [36]. In the crystal 8A, a different orientation of the ester group may be caused by the presence of the propargyl moiety with the acetylene labile hydrogen atom which may be involved in weak intermolecular hydrogen bonds with the oxygen atom of the hydroxyl group at C3 (C33–H33···O1) (see Table 3). The different orientation of the ester group on carbon C17 is depicted in Fig. 3 as a superposition of molecules **4** and **8A**.

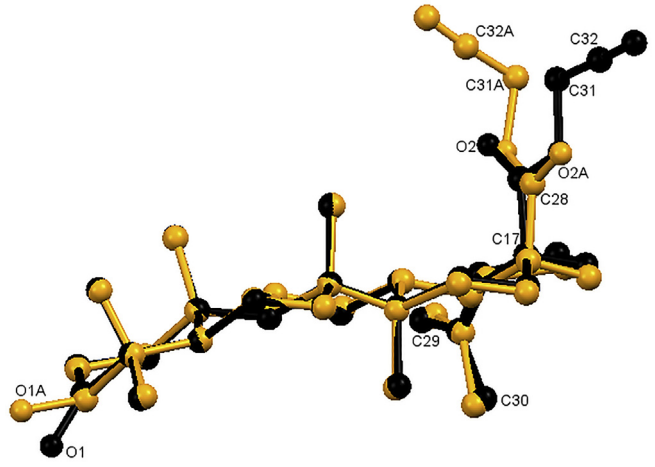

Fig. 3. Superposition of molecules **4** (black) and **8A** (orange) (For interpretation of the references to color in this figure legend, the reader is referred to the web version of this article.).

The extended structures **4** and **8A** in both crystal lattices are stabilized by intermolecular hydrogen bonds and van der Waals interactions. Additionally, some intramolecular H-bonds are also observed. The C13–H13···O2 and C19–H19···O3 are the intramolecular interactions involving the carbonyl group of the ester moiety in the crystal **4** and **8A**, respectively (see Table 3).

The molecules of both propargyl derivatives, **4** and **8A**, have different arrangements in the unit cell. In the compound **4**, the molecules are connected by weak hydrogen bonds C30-H30 B···O1, so-called head to tail (see Fig 4a). These connections form an infinite counterclockwise spiral along the *a*-axis, stabilized by the interactions of C33–H33···O2, as shown in Fig 4b. Moreover, the neighboring spirals are linked by weak C31–H31A···O1 and C24–H24 B···O1 interactions. The view of the spirals arrangement in the *bc* plane is presented in Fig. 5.

The replacement of the carbonyl group at the position C3 of the compound **4** by the hydroxyl group changes arrangement of molecules, as observed in the crystal structure of **8A**.

The main difference between the crystals **4** and **8A** (as a solvate) is the presence of DMF molecules in the structure. The ester molecules are connected by intermolecular C33–H33···O1 H-bonds, so-called head to tail, forming the counterclockwise spirals along the *a*-axis, similarly to those in the crystal **4**. Additionally, the DMF molecules are involved in O1–H1···O4 H-bonds with hydroxyl groups at C3 position. The view of the spiral arrangement in the *bc* plane, including the solvent molecules, is presented in Fig. 6.

The spirals of the crystal **8A** are joint together by DMF molecules via C36–H36···O1 H-bonds, as shown in Fig 7a. These interactions additional stabilize the three-dimensional network in the crystalline structure of compound **8A** (see Fig 7b).

4.3. Differential scanning calorimetry (DSC)

Thermal analysis was performed by means of differential scanning calorimetry DSC, measuring the heat flow in a function of linearly increasing temperature.

Fig. 8a shows the heat flow versus temperature for the compound number **4**. One may observe two main thermal events. The first one is an exothermal peak occurring at 56 °C. A similar exothermal peak for betulonic acid [37] and for oleanoic acid solvates [38] was reported. Such effect can be attributed to some structural relaxations and/or atomic reorientations. The second thermal effect is an endothermic peak at the temperature of 168.7 °C and is related to the melting point of the measured compound.

Table 3
Parameters (Å, degree) of the H-bonds for propargyl betulonate **4** and propargyl betulinate **8A**.

	D-H···A	D–H	H···A	D···A	<(DHA)
4	C13–H13···O2	0.97(2)	2.51(2)	3.158(2)	123.6(15)
	C30–H30 B···O1^{i}	1.02(3)	2.41(3)	3.370(3)	156.1(18)
	C31–H31A···O1^{ii}	1.02(2)	2.50(2)	2.917(2)	103.5(15)
	C24–H24 B···O1^{iii}	1.00(2)	2.65(2)	3.422(3)	134.4(18)
	C33–H33···O2^{iv}	0.91(2)	2.65(2)	3.464(3)	149.6(19)
8A	O1–H1···O4	0.89(3)	1.85(2)	2.705(3)	163(3)
	C19–H19···O3	1.02(3)	2.48(3)	2.904(3)	104.5(18)
	C23–H23 B···O1	0.99(3)	2.40(2)	2.883(4)	109(2)
	C33–H33···O1^{v}	0.99(3)	2.46(3)	3.432(4)	169(2)
	C35–H35 B···O4	1.00(3)	2.43(3)	2.804(4)	102(2)
	C36–H36C···O1^{vi}	1.06(3)	2.42(3)	3.438(4)	162(2)

Symmetry codes: i: 1/2 + x,1/2–y, 1–z; ii: 1/2–x,1–y,–1/2 + z; iii: 1/2 + x, 3/2–y, 1–z; iv: 1 + x, y, z; v: –1/2 + x,3/2–y,2-z; vi: 1/2 + x,1/2–y,2-z.

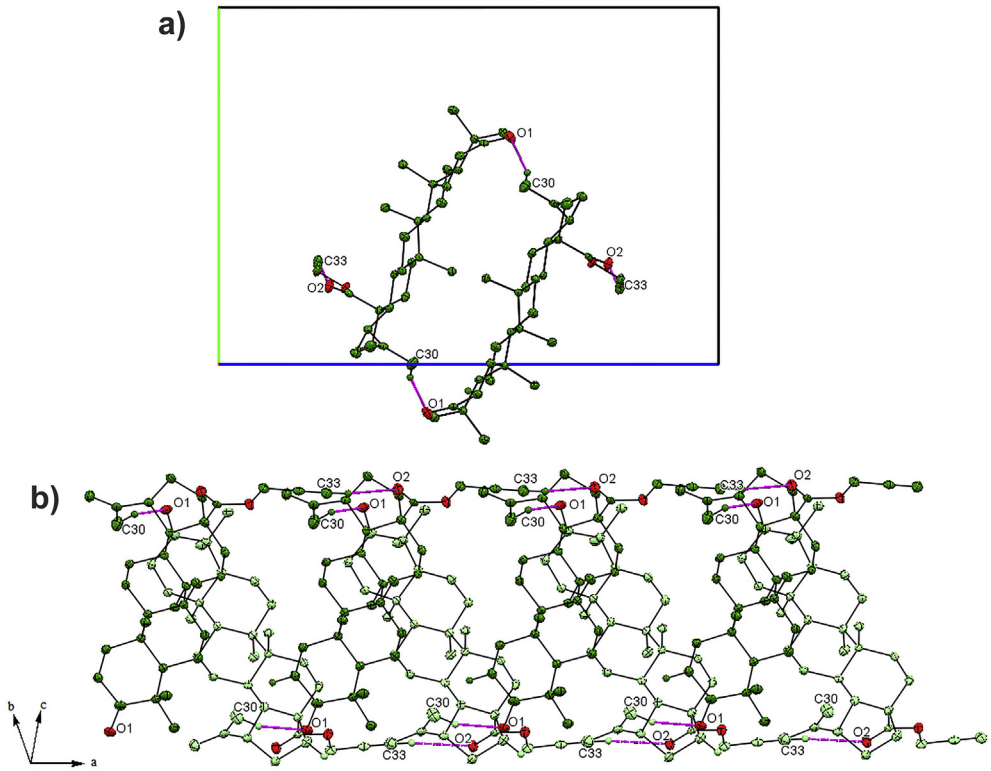

Fig. 4. a) Representation of hydrogen bonds in crystal **4**—view down *a*-axis, b) Spiral structure of ester **4** linked by weak H-bonds (H-bonds in purple) (For interpretation of the references to color in this figure legend, the reader is referred to the web version of this article.).

Fig. 8b presents similar DSC traces for the crystal **8** (without solvent) and **8A** (with solvent). For the compound **8** one additional endothermic peak, related to evaporation of the remaining solvent (ethanol) used in purification, was observed. The atomic reorientation and the melting point occurred at 37 °C and 186.5 °C, respectively. In the case of the crystal **8A** a significant shift of the melting temperature down to 121.1 °C is detected. Above this point a relatively broad endo-thermal peak caused by evaporation of DMF solvent is visible at 153 °C.

More detailed analysis of the melting events is presented in Fig. 9. In the all cases, symmetric Gaussian-like endothermic peaks are observed. From the area of the peaks and taking into consideration the applied heating rate one may determine values of melting enthalpy. The calculated values are 1.061 J/g, 0.867 J/g and 0.844 J/g for the crystals **4**, **8** and **8A**, respectively. In relation to **8** and **8A** one may conclude that the introduction of solvent into the

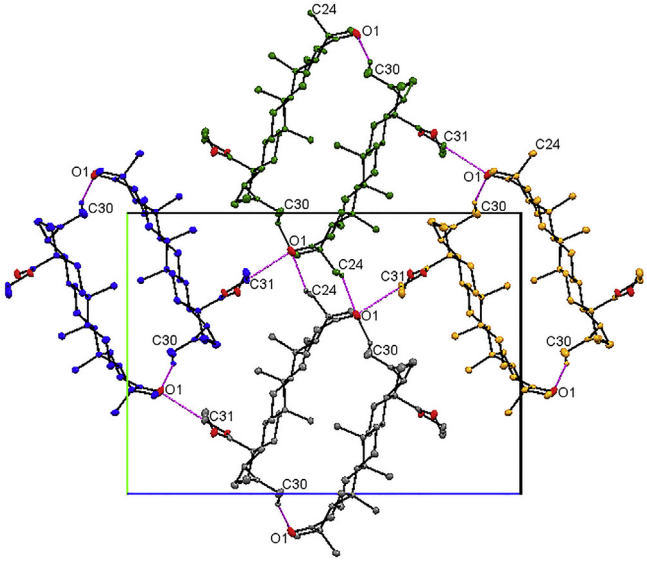

Fig. 5. Packing diagram of crystal **4** viewed parallel to the *a* −axis (C—H···O interactions in purple) (For interpretation of the references to color in this figure legend, the reader is referred to the web version of this article.).

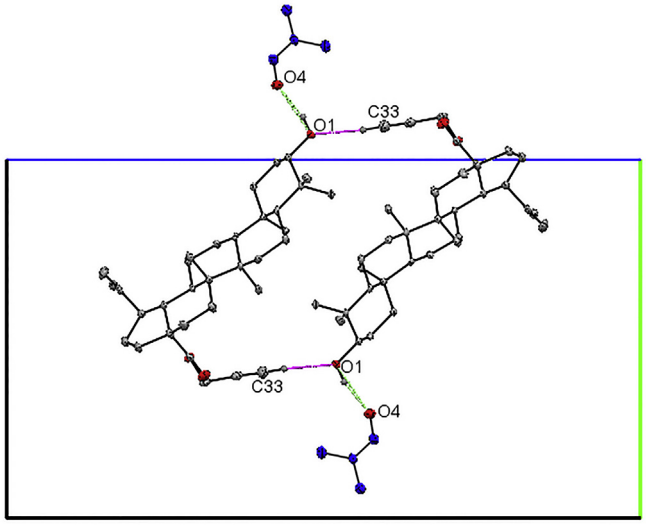

Fig. 6. Representation of hydrogen bonds in crystal **8A**—view down *a*-axis (O—H···O bonds in light green, C—H···O bonds in purple, molecules of *N,N*-dimethylformamide in blue) (For interpretation of the references to color in this figure legend, the reader is referred to the web version of this article.).

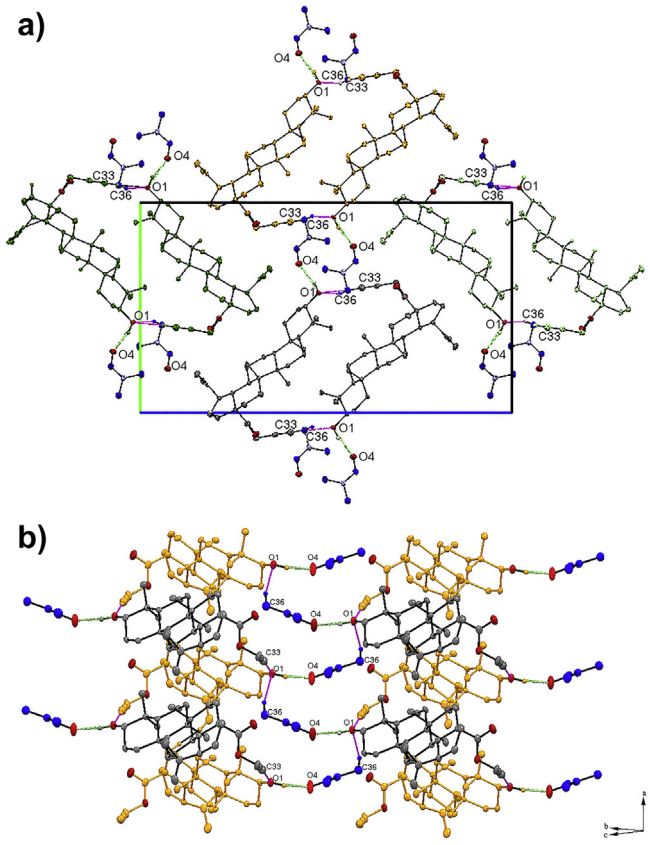

Fig. 7. a) Packing diagram and intermolecular H-bonds of crystal **8A** viewed parallel to the *a* −axis, b) Spiral structure and intermolecular H-bonds of crystal **8A** (O—H···O bonds in light green, C—H···O interactions in purple) (For interpretation of the references to color in this figure legend, the reader is referred to the web version of this article.).

crystal structure leads to a remarkable decrease of the melting temperature as well as lowering of melting enthalpy.

4.4. Cytotoxic activity

The studied compounds **4**–**11** were tested in SRB or MTT (in the case of leukemia cells) for their antiproliferative activity *in vitro* against human cancer lines: SW707 (colorectal adenocarcinoma), CCRF/CEM (leukemia), T47D (breast cancer) and murine P388 (leukemia) as well as BALB3T3 normal fibroblast cell lines. The results of the cytotoxic activity *in vitro* were signified as IC_{50} values (μg/mL). Cisplatin was used as a reference cytotoxic compound (positive test control). The antiproliferative activity criterion for the derivatives **4**–**11** was considered as a value of less than 4 μg/mL [39]. The results of the cytotoxicity studies are summarized in Table 4.

As shown in Table 4, the introduction of an acetylenic group at the C17 of betulonic and betulinic acids leads to a change of activity against the tested cancer lines, compared with betulin **1** and betulinic acid **3**. In the series of alkynyl derivatives **4**–**11**, the most active compound **8** was more cytotoxic than betulin **1** and betulinic acid **3** against the human CCRF/CEM (leukemia) cell line. Amide **11** exhibited high anticancer activity against the human T47D (breast cancer), SW707 (colorectal adenocarcinoma) and the mouse P388 (leukemia) cell lines. The compound **11** was four times more cytotoxic than betulin **1** against the human SW707 (colorectal adenocarcinoma) cell line. Replacement of the *O*-propargyl group by a propargylamide function (compounds **8** and **11**) had not significant effect on the cytotoxic activity against the cells of SW707, P388 and BALB3T3. Furthermore, this replacement led to a complete loss of activity against the CCRM/CEM cells. The cytotoxic activities of the synthesized compounds is dependent on the length of the alkynyl chain and position of the triple bond in the acetylene group. The obtained results also suggest that the compounds having shorter alkynyl chain are more cytotoxic to the tested cell lines. Moreover, the presence of the terminal triple bond is related to the good cytotoxic activity.

5. Conclusion

The present studies demonstrated that introduction of a substituent containing a triple bond at the carboxyl group is important for the cytotoxicity of the obtained betulonic and betulinic acids derivatives. Propargyl betulinate **8** and propargyl amide **11** were the most potent derivatives against the human breast cancer (SW707) and the mouse leukemia (P388) cell lines.

The performed DSC measurements reveal the occurrence of exothermal and endothermic effects attributed to some structural relaxation and melting point, respectively. In the case of 8.

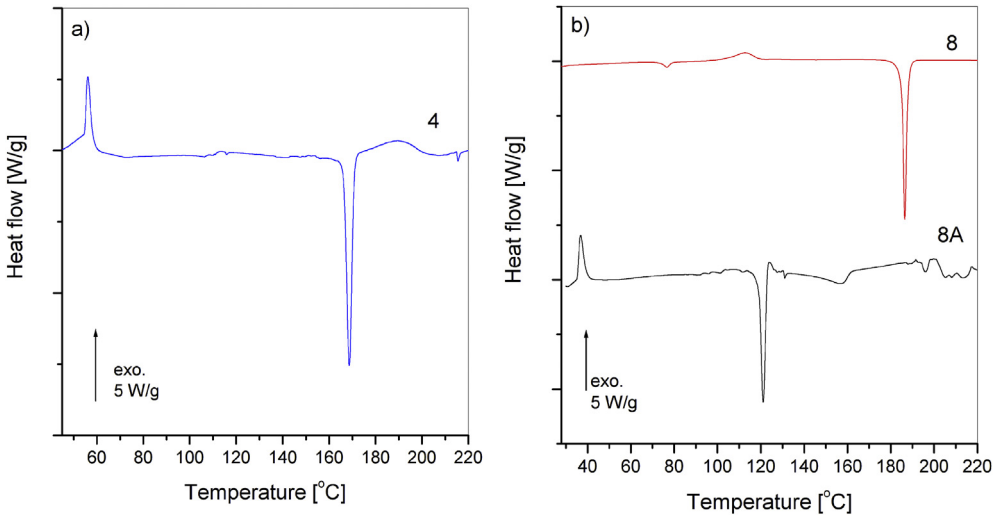

Fig. 8. DSC curves for crystals **4** (a), **8** and **8A** (b).

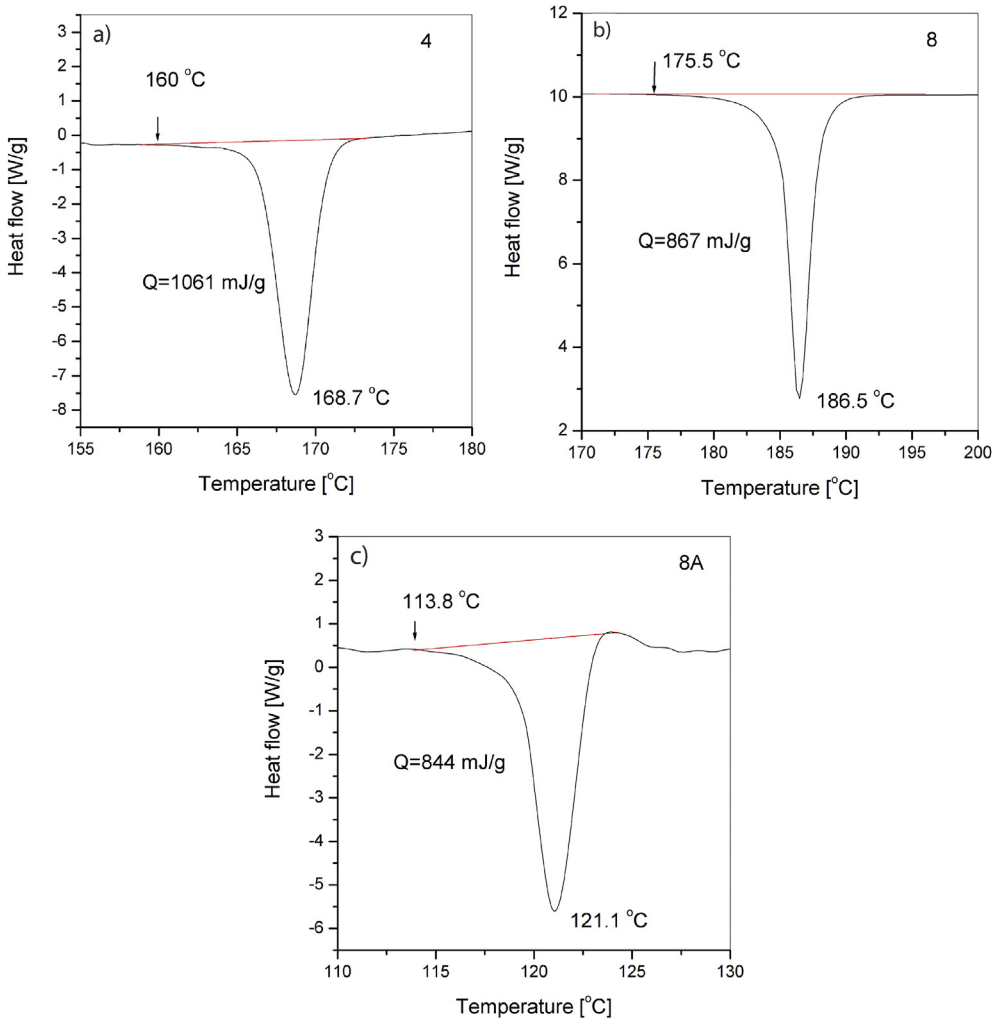

Fig. 9. DSC curves related to melting events for crystals **4** (a), **8** (b) and **8A** (c).

Table 4
Cytotoxic activity of betulin **1**, betulinic acid **3**, acetylenic derivatives **4**–**11** and cisplatin reference compound against the cells of the tested cancer cell lines.

Compound	Cytotoxic activity IC_{50} [μg/mL]				
	Human			Murine	
	T47D	CCRF/CEM	SW707	P388	BALB/3T3
Betulin 1	32.4 ± 10.7	10.9 ± 5.5	22.9 ± 15.4	5.5 ± 3.3	47.3 ± 7.9
Betulinic acid 3	5.4 ± 1.1	8.7 ± 2.6	13.2 ± 12.0	6.6 ± 3.9	26.5 ± 3.7
4	20.0 ± 6.7	9.1 ± 2.2	20.0 ± 20.4	15.1 ± 10.6	30.7 ± 3.1
5	Neg	44.6 ± 18.7	62.0 ± 1.8	34.9 ± 3.9	Neg
6	66.9 ± 24.3	36.3 ± 5.0	69.9 ± 21.0	35.4 ± 7.3	Neg
7	Neg	38.6 ± 9.9	Neg	25.5 ± 5.0	Neg
8	11.2 ± 7.7	3.9 ± 0.5	6.1 ± 1.5	6.7 ± 2.6	27.6 ± 6.4
9	29.8 ± 14.4	14.5 ± 11.5	21.2 ± 17.8	32.0 ± 1.7	37.2 ± 3.1
10	17.4 ± 3.1	5.7 ± 1.6	27.9 ± 18	24.5 ± 7.7	36.4 ± 2.2
11	6.2 ± 0.9	Neg	4.9 ± 0.6	5.1 ± 1.9	28.9 ± 5.8
Cisplatin	3.1 ± 1.0	2.0 ± 0.5	2.2 ± 0.5	0.5 ± 0.3	0.5 ± 0.3

Neg – negative in the concentration used.

and 8A, a significant decrease of melting temperature by about 65 K, related to the introduction of solvent into crystal structure, was observed.

Propargyl betulinate 8 forms a solvate with *N*,*N*-dimethylformamide during the crystallization process. In this crystal, the A-ring conformation and orientation of the ester group results from interactions of the carbonyl group and the terminal acetylenic hydrogen in intra- and intermolecular H-bonds, which stabilize the crystal structure.

Acknowledgments

This work was supported by the Medical University of Silesia in Katowice, Poland. Grant No KNW-1-002/N/5/0.

References

[1] S. Rastogi, M.M. Pandey, A.K.S. Rawat, Medicinal plants of the genus betula—traditional uses and a phytochemical-pharmacological review, J. Ethnopharmacol. 159 (2015) 62–83.

[2] Q.H. Chen, M.L. Fu, J. Liu, H.F. Zhang, G.Q. He, H. Ruan, Optimization of ultrasonic-assisted extraction (UAE) of betulin from white birch bark using response surface methodology, Ultrason. Sonochem. 16 (2009) 599–604.

[3] S. Alakurtti, T. Mäkelä, S. Koskimies, J. Yli-Kauhaluoma, Pharmacological properties of the ubiquitous natural product betulin, Eur. J. Pharm. Sci. 29 (2006) 1–13.

[4] G.A. Tolstikov, O.B. Flekhter, E.E. Shultz, L.A. Baltina, A.G. Tolstikov, Betulin and its derivatives. Chemistry and biological activity, Chem. Sustain. Dev. 13 (2005) 1–29.

[5] D.S.H.L. Kim, Z.D. Chen, V.T. Nguyen, J.M. Pezzuto, S.X. Qui, Z.Z. Lu, A concise semi-synthetic approach to betulinic acid from betulin, Synth. Comm. 27 (1997) 1607–1612.

[6] L. Pohjala, S. Alakurtti, T. Ahola, J. Yli-Kauhaluoma, P. Tammela, Betulin-derived compounds as inhibitors of alphavirus replication, J. Nat. Prod. 72 (2009) 1917–1926.

[7] R.C. Santos, J.A.R. Salvador, S. Marin, M. Cascante, J.N. Moreira, T.C.P. Dinis, Synthesis and structure–activity relationship study of novel cytotoxic carbamate and N-acylheterocyclic bearing derivatives of betulin and betulinic acid, Bioorg. Med. Chem. 18 (2010) 4385–4396.

[8] S.J. Yang, M.Ch Liu, Q. Zhao, D.Y. Hu, W. Xue, S. Yang, Synthesis and biological evaluation of betulonic acid derivatives as antitumor agents, Eur. J. Med. Chem. 96 (2015) 58–65.

[9] S. Boryczka, E. Bębenek, J. Wietrzyk, K. Kępińska, M. Jastrzębska, J. Kusz, M. Nowak, Synthesis, structure and cytotoxic activity of new acetylenic derivatives of betulin, Molecules 18 (2013) 4526–4543.

[10] R. Csuk, A. Barthel, S. Schwarz, H. Kommera, R. Paschke, Synthesis and biological evaluation of antitumor-active γ-butyrolactone substituted betulin derivatives, Bioorg. Med. Chem. 18 (2010) 2549–2558.

[11] O.B. Kazakova, G.V. Giniyatullina, E.Y. Yamansarov, G.A. Tolstikov, Betulin and ursolic acid synthetic derivatives as inhibitors of Papilloma virus, Bioorg. Med. Chem. Lett. 20 (2010) 4088–4090.

[12] R. Csuk, A. Barthel, R. Kluge, D. Ströhl, Synthesis, cytotoxicity and liposome preparation of 28-acetylenic betulin derivatives, Bioorg. Med. Chem. 18 (2010) 7252–7259.

[13] X. Wang, N. Gong, S. Yang, G. Du, Y. Lu, Studies on solvatomorphism of betulinic acid, J. Pharm. Sci. 103 (2014) 2696–2703.

[14] M.A. Mikhailenko, T.P. Shakhtshneider, M.E. Brezgunova, V.A. Drebushchak, S.A. Kuznetsova, V.V. Boldyrev, Khim. Rastit. Syr'ya 2 (2010) 63–70 (NIE MA TYTYŁU).

[15] H.G. Brittain, Polymorphism and solvatomorphism 2008, J. Pharm. Sci. 99 (2010) 3648–3664.

[16] H.G. Brittain, Polymorphism and solvatomorphism 2010, J. Pharm. Sci. 101 (2012) 464–484.

[17] S. Boryczka, E. Bębenek, M. Jastrzębska, J. Kusz, M. Zubko, Crystal structure of betulinic acid-DMSO solvate, Z. Krist. 227 (2012) 379–384.

[18] S. Boryczka, M. Jastrzębska, E. Bębenek, J. Kusz, M. Zubko, M. Kadela, E. Michalik, X-ray diffraction and infrared spectroscopy of N,N-dimethylformamide and dimethyl sulfoxide solvatomorphs of betulonic acid, J. Pharm. Sci. 101 (2012) 4458–4471.

[19] S. Boryczka, E. Michalik, M. Jastrzębska, J. Kusz, M. Zubko, E. Bębenek, X-ray crystal structure of betulin-DMSO solvate, J. Chem. Crystallogr. 42 (2012) 345–351.

[20] S.Z. Choi, M.Ch Yang, S.U. Choi, K.R. Lee, Cytotoxic terpenes and lignans from the roots of Ainsliaea acerifolia, Arch. Pharm. Res. 29 (2006) 203–208.

[21] A.I. Govdi, S.F. Vasilevsky, N.V. Sokolova, I.V. Sorokina, T.G. Tolstikova, V.G. Nenajdenko, Betulonic acid-peptide conjugates: synthesis and evaluation of anti- inflammatory activity, Mendeleev Commun. 23 (2013) 260–261.

[22] T.A. . Dang Thi, N.T. Kim Tuyet, C. Pham The, H. Thanh Nguyen, C. Ba Thi, T. Doan Duy, M. D'hooghe, T. Van Nguyen, Synthesis and cytotoxic evaluation of novel ester-triazole-linked triterpenoid-AZT conjugates, Bioorg. Med. Chem. Lett. 24 (2014) 5190–5194.

[23] T.A. . Dang Thi, N.T. Kim Tuyet, C. Pham The, H. Thanh Nguyen, C. Ba Thi, H. Thi Phuong, L. Van Boi, T. Van Nguyen, M. D'hooghe, Synthesis and cytotoxic evaluation of novel amide-triazole-linked triterpenoid-AZT conjugates, Tetrahydron Lett. 56 (2015) 218–224.

[24] Oxford Diffraction, CrysAlis CCD and CrysAlis RED. Version 1.171.32.29, Oxford Diffraction Ltd, Wrocław, 2008.

[25] G.M. Sheldrick, A short history of SHELX, Acta Cryst. A 64 (2008) 112–122.

[26] J. Wietrzyk, M. Chodyński, H. Fitak, E. Wojdat, A. Kutner, A. Opolski, Antitumor properties of diastereomeric and geometric analogs of vitamin D_3, Anticancer Drugs 18 (2007) 447–457.

[27] B.-N. Chen, G.-E. Yang, J.-K. Li, H.-J. Du, Q.-S. Li, Z.-M. Zang, Cytotoxic constituents from Viscum coloratum, Chem. Nat. Compd. 45 (2009) 547–549.

[28] G. Desiraju, T. Steiner, The Weak Hydrogen Bond: in Structural Chemistry and Biology, Oxford Uniwersity Press, 2001.

[29] P. Dampawan, C. Huntrakul, V. Reutrakul, C.L. Raston, A.H. White, Constituents of clinacanthus nutans and the crystal structure, J. Sci. Soc. Thail. 3 (1977) 14–26.

[30] E. Chrobak, E. Michalik, J. Kusz, M. Nowak, S. Boryczka, Polymorphic forms of lupane triterpenoid betulonic aldehyde (betulonal), Acta Cryst. C70 (2014) 847–851.

[31] T.N. Drebushchak, M.A. Mikhailenko, M.E. Brezgunova, T.P. Shakhtshneider, S.A. Kuznetsova, Crystal structure of betulin ethanol solvate, J. Struct. Chem. 51 (2010) 798–801.

[32] W. Tang, N.-H. Chen, G.-Q. Li, G.-C. Wang, Y.-L. Li, Crystal structure of betulinic acid methanol monosolvate, Acta Cryst. E70 (2014) o1242–o1243.

[33] R.S. Corrêa, C.P. Coelho, M.H. dos Santos, J. Ellena, A.C. Doriguetto, Lupeol, Acta Cryst. C65 (2009) o97–o99.

[34] G. Bringmann, W. Saeb, L.A. Assi, G. Francois, A.S.S. Narayanan, K. Peters, E.M. Peters, Betulinic acid: isolation from Triphyophyllum peltatum and Ancistrocladus heyneanus, antimalarial activity, and crystal structure of the benzyl ester, Planta Med. 63 (1997) 255–257.

[35] G.V. Giniyatullina, O.B. Flekhter, I.P. Baikova, Z.A. Starikova, G.A. Tolstikov, Effective synthesis of methyl 3β-amino-3-deoxybetulinate, Chem. Nat. Compd. 44 (2008) 603–605.

[36] C. Genet, C. Schmidt, A. Strehle, K. Schoonjans, J. Auwerx, R. Saladin, A. Wagner, Redefining the TGR5 triterpenoid binding pocket at the C-3 position, Chem. Med. Chem. 5 (2010) 1983–1988.

[37] C. Soica, C. Danciu, G. Savoiu-Balint, F. Borcan, R. Ambrus, I. Zupko, F. Bojin, D. Coricovac, S. Ciurlea, S. Avram, C.A. Dehelean, T. Olariu, P. Matusz, Betulinic acid in complex with a gamma-cyclodextrin derivative decreases proliferation and in vivo tumor development of non-metastatic and metastatic B164A5 cells, Int. J. Mol. Sci. 15 (2014) 8235–8255.

[38] H.H.Y. Tong, H.B. Wu, Y. Zheng, J. Xi, A.H.L. Chow, C.K. Chan, Physical characterization of oleanolic acid nonsolvate and solvates prepared by solvent recrystallization, Int. J. Pharm. 355 (2008) 195–202.

[39] R.I. Geran, N.H. Greenberg, M.M. Macdonald, A.M. Schumacher, B.J. Abbott, Protocols for screening chemical agents and natural products against animal tumors and other biological systems, Cancer Chemother. Rep. 3 (1972) 59–72.